

ОБЪЕДИНЕННЫЙ
ИНСТИТУТ
ЯДЕРНЫХ
ИССЛЕДОВАНИЙ
ДУБНА



3630/2-76

13/12-76

E1 - 9781

B-77

**SINGLE-PARTICLE INCLUSIVE SPECTRA
OF CHARGED PARTICLES
IN $\bar{p}p$ - INTERACTIONS AT 22.4 GEV/C**

**Alma-Ata - Dubna - Helsinki - Košice -
Moscow - Prague Collaboration**

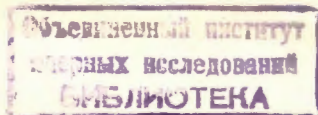
1976

EI - 9781

**SINGLE-PARTICLE INCLUSIVE SPECTRA
OF CHARGED PARTICLES
IN $\bar{p}p$ - INTERACTIONS AT 22.4 GEV/C**

**Alma-Ata - Dubna - Helsinki - Košice -
Moscow - Prague Collaboration**

Submitted to "Nuclear Physics"



E.G.Boos, V.V.Samojlov, Zh.S.Takibaev,
M.A.Tashimov, T.Temiraliev

Institute of High Energy Physics, Alma-Ata,
USSR.

B.V.Batyunya, I.V.Boguslavsky, N.A.Buzdavina,
I.M.Gramenitsky, V.G.Ivanov, R.Lednicky,
L.A.Tikhonova, A.Valkarova, V.Vrba, Z.Zlatanov

Joint Institute for Nuclear Research, Dubna,
USSR.

I.Ervanne, S.Ljung, R.Orava, H.Villanen,
P.Villanen
Department of Nuclear Physics of the Helsinki
University, Helsinki, Finland.

J.Patočka
Institute of Experimental Physics, Košice,
CSSR

B.V.Korolev, Ya.M.Selektor, V.N.Shulyachenko,
V.F.Turov
Institute of Theoretical and Experimental
Physics, Moscow, USSR.

P.K.Dementiev, E.M.Lejkin, A.G.Pavlova,
N.A.Pozhidaeva, V.I.Rud

Institute for Nuclear Physics Research of
the Moscow University, Moscow, USSR.

L.Rob, J.Začek
Department of Physics and Mathematics of
the Karlov University, Prague, CSSR.

J.Böhm, J.Chyla, J.Cvač, I.Herinek,
P.Raimer, J.Sedlak, V.Šimák

Institute of Physics, Prague, CSSR.

1. Introduction

In this paper we present results on single-particle inclusive spectra of secondary charged particles produced in inelastic $\bar{p}p$ interactions at 22.4 GeV/c. The experimental data were obtained from the 2 m hydrogen bubble chamber "LUDMILA" exposed to a RF-separated anti-proton beam at the Serpukhov accelerator^{/1/}. Details of the scanning procedure and the beam characteristics were published earlier^{/2/}.

All events were measured using semi-automatic devices and processed by means of geometric reconstruction programs (MDTHRESH, HYDRA geometry). Visual estimates of ionization were made for all tracks of momentum less than 1.5 GeV/c. Necessary kinematic quantities were calculated and the data were recorded on DST by the program LINEX^{/3/}. Altogether 7343 inelastic events were used in this analysis*. Weights were introduced to account for scanning, measuring and computational losses. These weights vary with topology, the average value being equal to 1.26.

Losses due to slow recoil protons were estimated by fitting the $d\sigma/dt$ distribution by $A \exp(Bt)$. The interval $0.06 \leq |t| \leq 0.30$ (GeV/c)² gives $B = 12.0 \pm 0.6$ (GeV/c)². This agrees with the value at 25.2 GeV/c from ref.^{/4/} ($B = 11.8 \pm 0.1$) for pp interactions. We also used the azimuthal angle distributions of the slow proton for various values of t and the constraint

$$\Delta_{el} = [\sigma_{el} N_{tot} - (\sigma_{tot} - \Delta_{in}) N_{el}] / (N_{tot} - N_{el}).$$

* 1175 elastic events were excluded. For these events the missing mass to the identified proton was required to be less than 1.15 GeV and the laboratory momentum of the negative particle greater than 19 GeV/c.

Thus the losses were found to be $\Delta_{el} = 2.6 \pm 0.2 \text{ mb}$ for elastic events and $\Delta_{in} = 0.30 \pm 0.05 \text{ mb}$ for inelastic events. Taking all corrections into account, our microbarn equivalent is equal to $4.60 \pm 0.05 \text{ } \mu\text{b}$ per event.

2. Momentum Distributions

The momentum distributions for positive and negative particles in the laboratory frame are shown in *fig. 1*

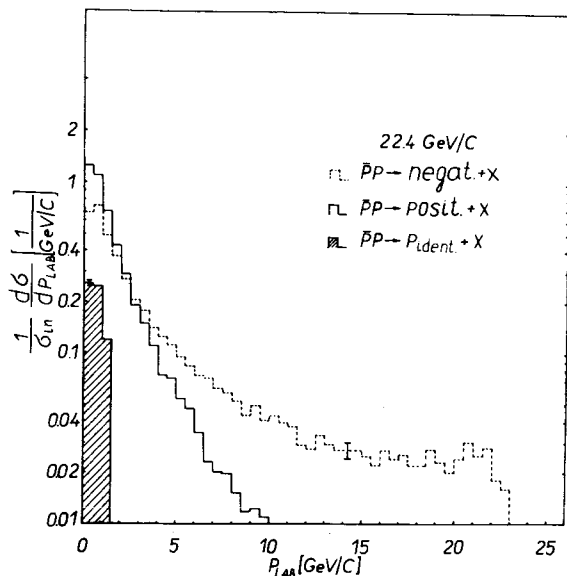


Fig. 1. The laboratory momentum distributions of secondary particles produced in $\bar{p}p$ interactions at 22.4 GeV/c.

together with those for identified protons. A peak at large momenta of negative particles indicates the presence of fast antiprotons and is mostly related to diffraction dissociation. The transverse momentum squared distributions for negative and positive tracks as well as for identified protons are given in *fig. 2*. As is seen from

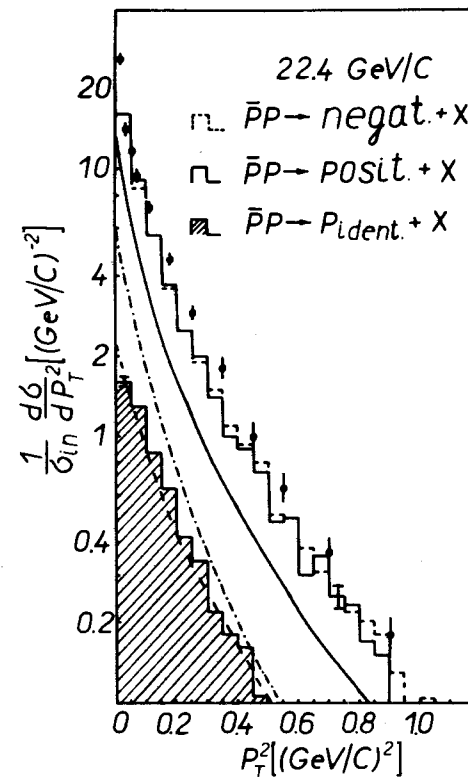


Fig. 2. The distributions of the transverse momentum squared. The solid line and the dash-dotted line show the distributions for the reaction $pp \rightarrow \pi^- + X$ at 205^{/7/} and 28.5 GeV/c^{/6/}, respectively, the dashed line, the reaction $pp \rightarrow p + X$ at 205 GeVc^{/7/} ($-1.5 \leq x \leq -0.5$), the points, the reaction $\bar{p}p \rightarrow \pi^+ + X$ at 100 GeV/c

Table 1, these distributions are well fitted by the two-exponential expression

$$\frac{d\sigma}{dp_T^2} = a \exp(-b_1 p_T^2) / I_1 + (1-a) \exp(-b_2 p_T^2) / I_2,$$

where $I_{1,2}$ are the normalization integrals. Note that the p_T^2 distributions for the 22.4 and 100 GeV/c $\bar{p}p$ data^{/5/} are similar in shape, our data being slightly lower due

Table 1

Mixing parameter and slopes obtained in the two-exponential fit of the p_T^2 distributions

Particle	p_T^2 (GeV/c) ²	Parameters			χ^2/ND
		α	b_1 (GeV/c) ⁻²	b_2 (GeV/c) ⁻²	
positive	0.04 - 1.0	0.45 ± 0.04	13.1 ± 0.8	3.9 ± 0.2	57.5/44
p	0.04 - 1.0	0.24 ± 0.10	17.1 ± 5.0	5.6 ± 0.4	39.6/44
+	0.0 - 1.0	0.51 ± 0.03	15.2 ± 0.7	4.1 ± 0.2	70.2/46
negative	0.0 - 1.0	0.48 ± 0.03	15.3 ± 0.7	4.0 ± 0.1	45.3/46

to smaller multiplicity of secondary particles. To compare our results with pp data, we present in *fig. 2* also the p_T^2 distributions obtained for the 28.5 and 205 GeV/c pp data^{/6,7/}. There is a close agreement between our spectrum for identified protons and that from the 205 GeV/c pp data. The statistical parameters of the transverse momentum spectra of charged particles, along with the results of other experiments, are given in *Table 2*. The average values of the p_T and p_T^2 distributions of positive and negative particles are close to those for π^- in the $pp \rightarrow \pi^- + X$ reaction at 102 and 205 GeV/c^{/7/}. It should be noted that the values of $\langle p_T \rangle$ and $D = (\langle p_T^2 \rangle - \langle p_T \rangle^2)^{1/2}$ for negative pions produced in the reactions $pp \rightarrow \pi^- + X$, $\pi^+ p \rightarrow \pi^- + X$, $K^+ p \rightarrow \pi^- + X$, etc., increase logarithmically with energy up to 100 GeV^{/8/} and eventually reach a plateau at about 200 GeV^{/7/}.

The average transverse momentum for positive pions from events with an identified proton is $\langle p_T \rangle = 0.292 \pm 0.004$ *. It is equal to the average p_T value at 12 GeV/c for charged pions in the non-annihilation channels of the reaction $pp \rightarrow \pi + X$ ^{/9/}.

3. Upper Limit for the Antiproton Diffraction Dissociation Cross Section

Dissociation of the target or the beam particle is an important feature of high energy collisions. For example, in the reaction $pp \rightarrow p + X$ there is an enhancement at low missing mass values ($M_X^2 < 5 \text{ GeV}^2$). The cross section for this enhancement depends weakly on energy, and the differential cross section $d\sigma/dt$ is similar to that of elastic scattering^{/7/}.

Figure 3 shows the missing mass squared distributions to the identified protons for different topologies in our experiment. For two-prong events there is a pronounced peak at about $M_X^2 \approx 2 \text{ GeV}^2$. For four-prong events such a peak is absent, and only some shoulder in this

* Only the statistical errors are taken into account.

Table 2
Average characteristics of transverse momenta

Reaction	Momentum GeV/c	Particle	$\langle p_T \rangle$ GeV/c	$\langle p_T^2 \rangle$ (GeV/c) ²	$D = (\langle p_T^2 \rangle - \langle p_T \rangle^2)^{1/2}$ GeV/c
$\bar{p}p$	22.4	positive	0.344 ± 0.003	0.170 ± 0.003	0.227 ± 0.003
		negative	0.354 ± 0.003	0.188 ± 0.003	0.250 ± 0.003
		π^+	0.342 ± 0.003	0.171 ± 0.003	0.232 ± 0.003
		p	0.357 ± 0.005	0.164 ± 0.004	0.172 ± 0.005
pp	102	π^-	0.343 ± 0.010	0.170 ± 0.010	0.228 ± 0.010
	205	π^-	0.343 ± 0.004	0.166 ± 0.003	0.220 ± 0.004

region is seen. For higher topologies this region is almost unpopulated. In Table 3 we compare the cross sections for the low mass enhancement ($M_X^2/s < 0.16$) in the reactions $\bar{p}p \rightarrow p + X$ at 22.4 and 32 GeV/c^{10/}. These cross sections are the same within two standard deviations, our values being, however, systematically higher.

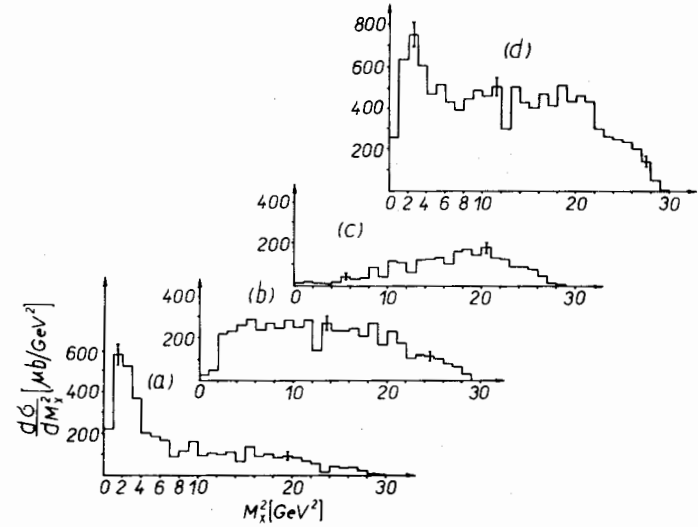


Fig. 3. The distributions of the missing mass squared to the identified proton a) for 2-prong events, b) for 4-prong events, c) for ≥ 6 -prong events, and d) for all topologies.

4. Single-Particle Distributions

The CMS rapidity distributions for positive and negative pions are shown in fig. 4 together with the data from the 14.75 and 100 GeV/c $\bar{p}p$ experiments ^{/11,5/}. The π^+ -meson distribution is reflected about $y^* = 0$, thus giving the corresponding distribution for π^- -mesons because of CP-symmetry. One can see that the cross

Table 3

Upper limits for the beam fragmentation cross sections

Prongs	$\bar{p}p \rightarrow p + X \ (M_X^2/s < 0.16)$	
	22.4 GeV/c	32.1 GeV/c
2	2.25 ± 0.41 0.11	1.8 ± 0.2
4	1.31 ± 0.09	1.1 ± 0.2
≥ 6	0.08 ± 0.02 0.45	0
all	3.68 ± 0.15	2.9 ± 0.3

* The error includes inelastic losses.

section in the central region is approximately the same in the energy interval from 15 to 100 GeV/c.

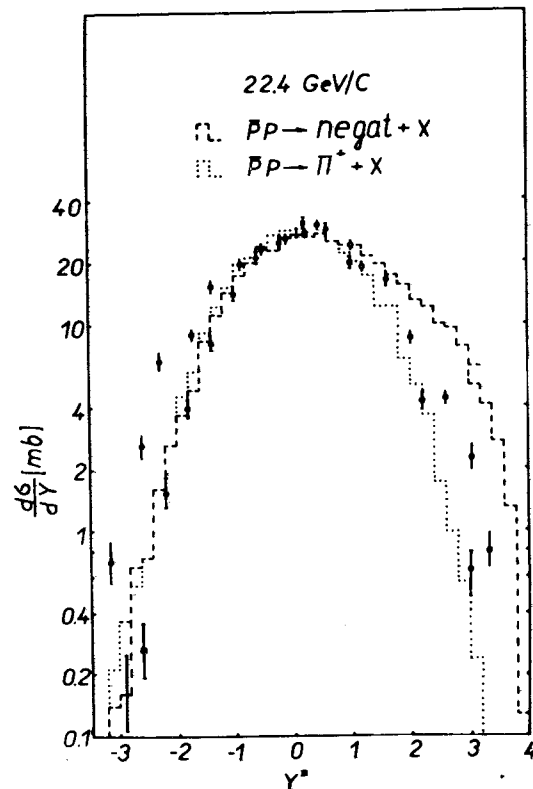


Fig. 4. The rapidity distributions in the CMS. The points show the distribution for the reaction $\bar{p}p \rightarrow \pi^+ + X$ at 100 GeV/c¹⁵⁾, the squares, for the reaction $\bar{p}p \rightarrow \pi^- + X$ at 14.75 GeV/c¹¹⁾. The distributions for π^+ -mesons are reflected about $y^* = 0$.

In fig. 5 the invariant cross section

$$f(x) = \int \frac{2E^*}{\pi\sqrt{s}} \cdot \frac{d^2\sigma}{dx dp_T^2} \cdot dp_T^2$$

is given (again the π^+ -distribution is reflected about $x = 0$) together with the data from the reactions $pp \rightarrow \pi^- + X$

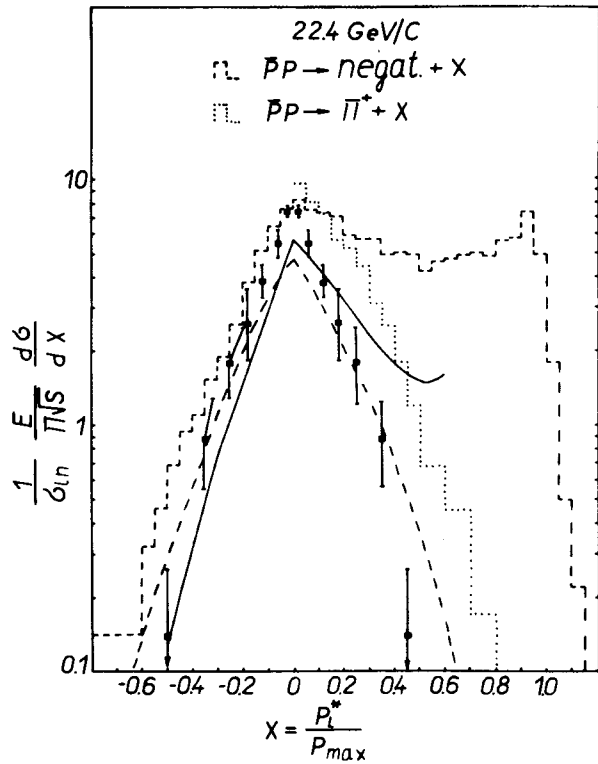


Fig. 5. The $f(x)$ distributions. The solid line shows the distribution for the reaction $\pi^- p \rightarrow \pi^- + X$ at $100 \text{ GeV}/c^{12/}$, the dashed line and the squares for the reaction $pp \rightarrow \pi^- + X$ at 28.5 and $102 \text{ GeV}/c^{6,7/}$. The distribution for π^+ -mesons is reflected about $x=0$.

at 28.5 and $102 \text{ GeV}/c^{6,7/}$ and $\pi^- p \rightarrow \pi^- + X$ at $100 \text{ GeV}/c^{12/}$. Our π^- distribution is close to that for pp interactions at $102 \text{ GeV}/c$ in the backward hemisphere.

The invariant cross section $\frac{1}{\sigma_{\text{tot}}} \frac{d\sigma}{dy^*}$ at $y^*=0$ is shown in fig. 6 together with results from other experiments as a function of $P_{\text{lab}}^{-1/4}$ ^{13/}. The invariant cross sections for $\bar{p}p \rightarrow \pi^- + X$ and $\pi^+ p \rightarrow \pi^+ + X$ are similar and weakly dependent on primary energy.

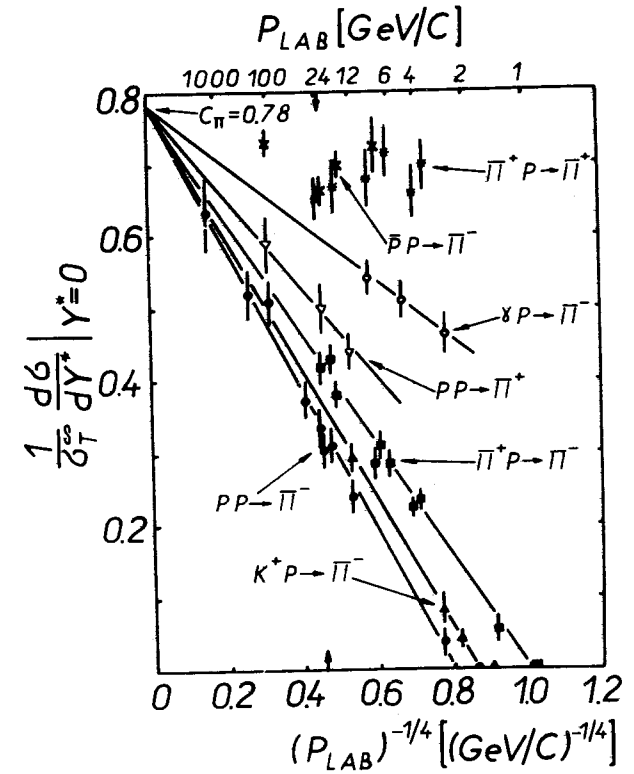


Fig. 6. The dependence of $\frac{1}{\sigma_{\text{tot}}} \frac{d\sigma}{dy} \Big|_{y^*=0}$ on $P_{\text{lab}}^{-1/4}$ for different inclusive reactions. The crosses correspond to the reaction $\bar{p}p \rightarrow \pi^- + X$ using the normalization $\sigma_{\text{tot}}(\bar{p}p) = 39.8 \text{ mb}^{13/}$.

In fig. 7 the target fragmentation cross sections $\frac{1}{\sigma_{\text{tot}}} \frac{d\sigma}{dy}$ at $y_{\text{lab}}=0$ are given for π^- -production from different initial states as functions of $s^{-1/2}$. A rapid decrease of the fragmentation cross section for the reaction $\bar{p}p \rightarrow \pi^- + X$ in the p interval from 4.5 to $22.3 \text{ GeV}/c$ fits the calculations done by Humble^{14/} on the basis of the multiperipheral model assuming a strong

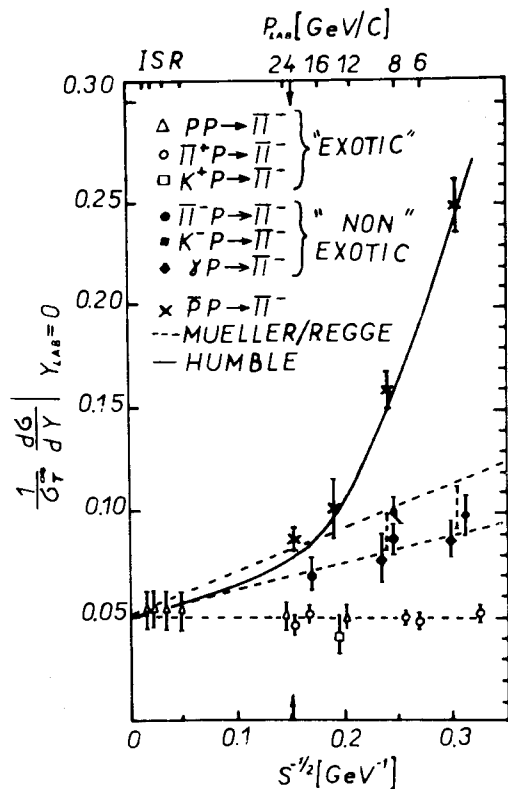


Fig. 7. The target fragmentation cross sections for different inclusive reactions as functions of $s^{-1/2}$.

energy dependence of the annihilation cross section and high multiplicities in the annihilation channels.

The x -distributions for negative and positive particles and identified π^+ -mesons are shown in fig. 8. The last two distributions are reflected about $x=0$. Note that the attribution of pion mass to a nucleon with $p_{lab} > 1.5 \text{ GeV}/c$ results in a positive shift of the value x , this shift being inversely proportional to the laboratory momentum of the particle, $\Delta x \approx 0.44 \text{ GeV}/c/p_{lab}$. This effect is negligible for x near 1 and becomes significant for $x \lesssim 0.2$ as indicated by the excess of po-

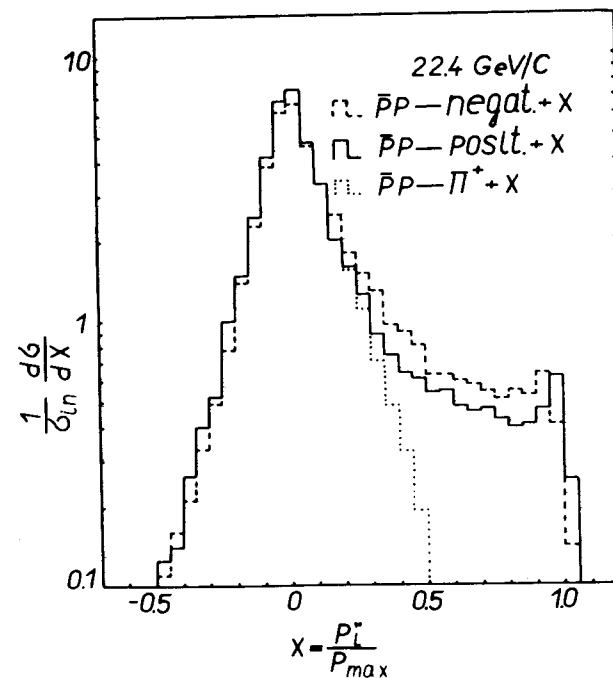


Fig. 8. The x distributions for negative and positive particles and π^+ -mesons. The two last distributions are reflected about $x=0$.

sitive particles over negative ones in the region of $x \approx 0$ and the opposite effect for $0.2 \lesssim x \lesssim 0.6$.

We also observe larger values of $\frac{1}{\sigma_{in}} \frac{d\sigma}{dx}$ for π^- in the forward hemisphere than in the backward one, particularly at small x , corresponding to the shift of the maximum in the y^* -distribution. To investigate this effect in more detail, we approximate the x distribution by $d\sigma/dx = A \exp(-b_+ |x|)$, separately for the forward (+) and backward (-) hemisphere for various intervals of p_T and x . The slopes decrease with growing p_T interval. Without any p_T cut $b_+ = 6.2 \pm 0.1$ and $b_- = 10.0 \pm 0.2$. The ratio of the slopes $R = b_-/b_+$ increases when broadening the x -interval and depends only weakly on the

transverse momentum. The values of R are close to 1.5 obtained in meson-nucleon interactions. This can be explained in a multiperipheral model by beam (target) charge transfer into the central region resulting in a characteristic shift of the maxima in the y^* -distributions^{/15/}. It is worth noting that the same shift can be obtained in a simple quark fusion model used for explanation of large p_T phenomena in pp -collisions^{/16/}. The ISR phenomena have been recently interpreted in a valence quark model^{/17/} assuming the dominance of the quark-diquark scattering amplitude. This model suggests a simple explanation at least of the high p_T part of the observed forward-backward asymmetry in $p\bar{p}$ interactions as well.

5. Conclusions

The main results of this analysis are summarized as follows:

(i) Average characteristics of the transverse momentum distribution show similar features as well as those from pp interactions at incident momenta higher than 100 GeV/c. There is an indication that $\langle p_T \rangle$ in annihilation reactions is essentially higher than in non-annihilation ones.

(ii) The upper limit of the antiproton diffraction dissociation cross section is (3.68 ± 0.45) mb. This value can be compared to (2.9 ± 0.3) mb achieved at 32 GeV/c incident momentum.

(iii) The c.m. rapidity distribution for pions is similar to those achieved at 14.75 and 100 GeV/c incident momenta but is more narrow than those at 100 GeV/c.

(iv) In the central region we see charge asymmetry. The asymmetry parameter is 0.15 ± 0.01 in the interval $0.00 \leq x \leq 0.16$.

Acknowledgement

The authors want to express their gratitude to the staff responsible for the operation of the Serpukhov accelerator and of the beam channel no. 9 and to the technical staff of the "LUDMILA" HBC. We also thank the technicians and assistants at all laboratories for their excellent work. The authors from the Moscow State University want to express their gratitude to Prof. V.G.Shevchenko for his continuous support of this work.

REFERENCES

1. V.N.Alferov et al. Preprint IHEP OP 74-53, Serpukhov, 1974.
V.N.Alferov et al. Preprint IHEP OP 74-54, Serpukhov, 1974.
K.I.Gubrienko et al. Preprint IHEP OP 74-55, Serpukhov, 1974.
2. L.N.Abesalashvili et al. Phys.Lett., 52B, 236 /1974/.
3. V.I.Rud, L.A.Tikhonova. Comm. JINR, 1-7671, Dubna, 1974.
4. Yu.M.Antipov et al. Nucl.Phys., B57, 333 /1973/.
5. Cambridge - Fermilab - Michigan State Collaboration. Analysis of Antiproton Reactions at 100 GeV/c, preliminary data, subm. to the Int. Conf. on High Energy Physics, Palermo, Italy, 1975.
6. W.H.Sims et al. Nucl.Phys., B41, 317 /1972/.
7. J.Whitmore. Phys.Rep., 100, No. 5 /1974/.
8. T.Ferbel. Proc. Int. Symp. on HEP, Tokyo /1973/.
9. D.Call. Proc. Int. Symp. on $p\bar{p}$ Interactions, Loma-Koli, Finland, June 11-19, 1975.
10. F.Grard et al. Phys.Lett., 59B, 409 /1975/.
11. F.T.Dao, J.Lach and J.Whitmore. Proc. Symp. on Antinucleon-Nucleon Inter., Lublice-Prague, June 25-28, 1974, p. 255; CERN 74-19, 1974.
12. G.A.Smith. Paper submitted to the 3d Int. Winter Meeting on Fundam. Physics, Parador se Sierra Nevada, Spain, Feb., 10-14, 1975, on behalf of the Fermilab, Iowa State, University of Maryland, Michigan State Univ. Collaboration.
13. T.Ferbel. Phys. Rev. Lett., 29, 448 /1972/.
14. S.Humble. CERN Th 1830, 1974.
15. A.K.Likhoded, A.N.Tolstenkov. Preprint IHEP 74-51, Serpukhov, 1974.

16. P.V.Landshoff, J.C.Polkinghorne. *Phys. Rev.*, D8, 4157 /1973/; *Phys. Rev.*, D10, 891 /1974/.
17. J.C.Polkinghorne. *Phys.Lett.*, 60B, 281 /1976/.

Received by Publishing Department
on May 12, 1976.

Боос Э.Г., Самойлов В.В., Такибаев Ж.С. и др.

E1 - 9781

Анализ инклюзивных распределений в $\bar{p}p$ -взаимодействиях при 22,4 ГэВ/с

Приведен анализ инклюзивных спектров при взаимодействии антипротонов с протонами при 22,4 ГэВ/с. Получены распределения по поперечному импульсу, инвариантные сечения и оценена зарядовая асимметрия в центральной области. Произведена также оценка сечения дифракционной диссоциации.

Работа выполнена в Лаборатории высоких энергий ОИЯИ.

Препринт Объединенного института ядерных исследований
Дубна 1976

Boos E.G., Samojlov V.V.,
Takibaev Zh.S. et al.

E1 -9781

Single-Particle Inclusive Spectra of Charged
Particles in $\bar{p}p$ Interactions at 22.4 GeV/c

The inclusive spectra for $\bar{p}p$ collisions at 22.4 GeV/c are investigated. The transverse momentum distribution resembles the corresponding one in high energy pp interactions. The cross section in the central region is 28 ± 1 mb. The y^* distributions of secondary particles in the central region indicates a charge asymmetry with the asymmetry parameter having the value 0.15 ± 0.01 . The upper limit of the diffraction dissociation of the beam particle is estimated to be $(3.68_{-0.15}^{+0.45})$ mb.

Preprint of the Joint Institute for Nuclear Research

Dubna 1976